PAPER

Check for updates

Single particle ICP-MS: a tool for the characterization of gold nanoparticles in nanotheranostics applications†

Meritxell Cabré, [ab] Gabriel Fernández, [a] Esther González, [a] Jordi Abellà [a] and Ariadna Verdaguer *[a]

Nanotheranostics aims to perform a premature and non-invasive diagnosis combined with therapy focused on the specific place where the disease is by using nanomaterials. To evaluate the ability to penetrate and retain the inorganic nanoparticles (NPs) in the cells, analytical techniques such as Single-Particle ICP-MS (SP-ICP-MS) are required to characterize these NPs. SP-ICP-MS provides not only the size distribution and concentration of NPs but also the concentration of the dissolved elements. In recent years, direct alkaline dilution of blood, serum, and urine is performed in clinical laboratories for routine analysis. This alkaline diluent is named clinical diluent and it is a mixture of ammonia, EDTA, 2-propanol, Triton X100, and purified water. In this work, a methodology to characterize AuNPs in blood and urine samples using SP-ICP-MS has been developed. Samples were directly diluted with clinical diluent before multi-quadrupole ICP-MS analysis. The effect of this clinical diluent on the behaviour and stability of AuNPs has been studied. Good stability of AuNPs was observed for both the particle size and particle concentration (<17% difference in 10 days). Moreover, analytical parameters of this method such as linearity, detection limit, accuracy, and precision in blood and urine samples were studied for both the particle size and particle concentration. Linearity was evaluated for particle size (from 10 to 100 nm) and particle concentration (from 5×10^3 to 1×10^4 NP per mL). Furthermore, recoveries between 88% and 103% for the NP concentration and between 100% and 110% for the nanoparticle size were obtained. Dissolved and gold nanoparticle detection limits have also been estimated.

1. Introduction

The term nanomedicine emerged in the 1990s.[1] This branch of science aims to harness advances in nanotechnology to address complex challenges in disease detection, drug delivery, and therapeutic efficacy. To achieve these goals, nanomaterials such as liposomes or nanoparticles have been used. These materials have physicochemical properties that allow them to interact with biological systems at the cellular and molecular levels. Nanotheranostics is a specialised branch of nanomedicine that focuses on the development of nanoplatforms that integrate therapy and diagnosis into a single system. There are different nanoplatforms such as micelles, carbon nanotubes, liposomes, dendrimers, and inorganic nanoparticles, among others.[2]

Particularly, inorganic nanoparticles (NPs) have unique mechanical, optical, magnetic, electric, and structural properties due to their size (from 1 to 100 nm) and surface/volume ratio.[3–5] Furthermore, at the nanoscale, the particles are more bioactive and more chemically active, allowing easy entry into the cells and organs. Therefore, NPs hold great potential for use in nanotheranostics as they allow real-time monitoring of how the drug gets delivered and distributed.

Nanotheranostics studies are performed using different nanoparticle compositions and size distribution depending on the target disease. Some of the most commonly used nanoparticles are gold, silver, titanium IV oxide, zinc II oxide, cerium IV oxide, and iron oxides.[6] Due to their optical properties, gold nanoparticles (AuNPs) are used as contrast agents in diagnostics. In addition, their plasmonic properties allow AuNPs to be used as diagnostic and therapeutic agents. Furthermore, their photothermal properties can be applied in therapeutic applications and their biocompatibility as drug delivery systems.[2–9] Thus, gold nanoparticles can be widely used in nanotheranostics applications. Since these NPs will be introduced into the body, it is important to have analytical techniques for the characterization of these nanoparticles and their interaction with cells. The characterization of these NPs will provide information on their bioavailability, their transport in the body,

[a]Analytical and Applied Chemistry Department, IQS School of Engineering, Ramon Llull University, Via Augusta 390, 08017 Barcelona, Spain. E-mail: ariadna.verdaguer@iqs.url.edu

[b]PerkinElmer Scientific Spain, S.L., Ronda de Poniente 19, 28760 Tres Cantos, Spain

† Electronic supplementary information (ESI) available. See DOI: https://doi.org/10.1039/d4ja00141a

their excretion, and whether these NPs transform when inside the organism.

Currently, these nanoparticles can be characterized by several techniques. These include Transmission Electron Microscopy (TEM), Scanning Electron Microscopy (SEM), Dynamic Light Scattering (DLS), Nanoparticle Tracking Analysis (NTA), Single Particle ICP-MS (SP-ICP-MS) and Asymmetric Flow Field-Flow Fractionation coupled to ICP-MS (AF4-ICP-MS), among others.[6,10–15] Each of these techniques provides relevant information about the nanoparticles, but each has its own limitations. For example, TEM and SEM supply details about the structure, shape, size, and composition of the nanoparticles. However, preparing the sample is time-consuming and only allows a small portion of the sample to be examined. They also do not give information about the concentration of NPs. In contrast, DLS and NTA offer information about nanoparticle hydrodynamic diameter and concentration but also have some limitations such as lack of selectivity, low sensitivity, and polydispersity. Thus, more techniques are needed to obtain information regarding both the nanoparticle size and concentration.

In 2003, Degueldre et al. first described the basic principles of SP-ICP-MS.[16] Since then the ICP-MS equipment has undergone improvements. Today's detectors analyse faster, allowing dwell time values to be reduced to 10 μs. Furthermore, this new generation of instruments offers increased sensitivity, facilitating the characterization of smaller nanoparticles. With its high selectivity and specificity, this technique holds great promise for nanoparticle characterization. Compared to other techniques, SP-ICP-MS provides not only the size distribution and the concentration of NPs but also the concentration of the dissolved element in the suspension.[13–15,17–24] This technique can therefore reveal relevant information on inorganic nanoparticle behaviour, which will help to understand how NPs are transported within the body and how they are excreted. However, there are only a few studies where this technique has been used to obtain such information.[6,12,25,26]

The metal content of biological fluids is routinely measured in clinical analytical laboratories. Due to the complex nature of the matrix, the clinical diluent is widely used. This is an alkaline solution that offers several advantages in the analysis of biological samples such as blood and urine. Firstly, the clinical diluent facilitates erythrocyte lysis, a crucial step in the sample preparation that ensures efficient extraction of target analytes. In addition, alkaline solutions prevent precipitation, reducing the risk of nebuliser clogging during analysis. They also help to mitigate memory effects and minimise spectral and matrix interferences, enhancing the accuracy and reliability of subsequent measurements. In summary, the use of alkaline solutions simplifies sample preparation, improves analytical performance and increases the robustness of analytical methods.[25]

The aim of this work is to provide new methodologies to characterize nanoparticles in the blood and urine of living organisms involved in nanotheranostics applications by SP-ICP-MS. To achieve this, we propose to investigate the feasibility of sample preparation by direct dilution of blood and urine using clinical diluent. All experiments were performed in accordance with the Guidelines of Spanish Biomedical Research Law 14/2007, and experiments were approved by the ethics committee at Ramon Llull University (approved ethical protocols CER_URL_2019_2020_016 and 200039). Samples were obtained from healthy volunteers who gave their informed consent.

2. Materials and methods

2.1. Standards and reagents

Clinical diluent was prepared with 0.5 g of EDTA, 10 mL isopropyl alcohol, 10 mL Ammonia solution, 0.5 g Triton-X100 and filled up to 1 L Milli-Q water. This clinical diluent was used to dilute all standard solutions. Ethylenediaminetetraacetic acid (EDTA for analysis, ref. 131026.1210) was supplied by Panreac. Isopropyl alcohol (HPLC grade, ref. P/7507/17) was purchased from Fisher Scientific. Ammonia solution (25%, ref. 1.05428) was supplied by Merck. Triton-X100 was supplied by Sigma Aldrich.

Gold standard solution (1000 mg L^{-1}, ref. N9303759) was supplied by PerkinElmer. Gold nanoparticle standard solutions with nominal sizes of 10 nm (9.1 ± 0.8), 20 nm (20.8 ± 1), 30 nm (27.1 ± 2.2), 50 nm (49.6 ± 4.2) and 100 nm (99.4 ± 6) were purchased from NanoComposix, Inc (San Diego, USA).

2.2. Instrumentation

A PerkinElmer NexION® 5000 (PerkinElmer, Waltham, USA) was used for this study. This ICP-MS is equipped with four quadrupoles to guide the ions generated in the plasma and to suppress interferences. The sample introduction system consists of a PFA nebulizer and a quartz cyclonic spray chamber. The sample flow rate was determined daily as the difference in weight after 4 minutes of uptake. A 50 nm gold nanoparticle suspension (10^4 NPs per mL) was prepared in clinical diluent to determine the transport efficiency (TE%). The mean of two measurements was used for sample analysis.

Homogenisation of the nanoparticle suspension prior to dilution was performed in an ultrasonic bath (J. P. Selecta, S.A.).

2.3. Sample preparation

2.3.1. AuNPs stability test. The 50 nm AuNP standard was diluted to 10^4, 5×10^4 and 10^5 NPs per mL with clinical diluent. These solutions were prepared in triplicate and stored at 5 ± 3 °C for 10 days.

2.3.2. Sample collection. In this study, blood and urine samples were collected from healthy donors and stored at 5 °C.

2.3.3. Blood samples. 0.2 mL of blood sample was diluted to 4 mL with clinical diluent. Moreover, 50 nm AuNP standard at three concentration levels were added to the blood sample to obtain a final nanoparticles concentration of 10^3, 5×10^3 and 10^4 NPs per mL. Three replicates of each solution were prepared.

2.3.4. Urine samples. 0.4 mL of the urine sample was diluted to 4 mL with clinical diluent. Furthermore, 50 nm AuNP standard at three concentration levels was added to urine samples to obtain a final nanoparticles concentration of 10^3, 5

This journal is © The Royal Society of Chemistry 2024

J. Anal. At. Spectrom., 2024, 39, 2508–2513 | 2509

$\times 10^3$ and 10^4 NPs per mL. Three replicates of each solution were prepared.

3.   Results and discussion

3.1.   Instrumental method optimization

The use of single quad (Q3 only: 197 m/z) and tandem quad (MS/MS: 197/197 m/z) was evaluated for gold nanoparticle characterization. A 2 µg L^{-1} dissolved gold solution and 50 nm gold standard nanoparticle solutions prepared in clinical diluent were analysed under both conditions (ESI Table S1†). For both solutions, higher mean intensities were obtained in Q3 only mode compared to MS/MS (266 and 59 mean AuNP counts, respectively). Nevertheless, no differences in nanoparticle size and concentration were observed. Thus, MS/MS is sensitive enough to characterize gold nanoparticles with a nominal size of 50 nm.

Once the acquisition mode is optimized the dwell time was evaluated as described in other studies.[18,27] In this case it was carried out with a suspension of gold nanoparticles of 50 nm. The dwell time values studied were: 20, 50, 100, 500 and 1000 µs obtaining transient signals (ESI Fig. S1†). As indicated in the literature, longer dwell times result in fewer events defining the peak. Therefore, a dwell time of 50 µs was chosen. This ensures a well-defined peak, minimising double nanoparticle events and providing sufficient sensitivity for this study. The optimised conditions for the characterization of gold nanoparticles are summarised in Table 1.

3.2.   Analytical parameters evaluation

The analytical parameters including linearity and detection limit for dissolved gold, and both nanoparticle size and concentration were evaluated.

Good linearity was observed for the dissolved gold within the concentration range of 1 to 5 µg L^{-1}, with a coefficient of determination higher than 0.995. Furthermore, a detection limit of 0.012 µg L^{-1} was determined, calculated as the 3-fold standard deviation of 10 blank measurements.

To assess the linearity of the nanoparticle size, suspensions of different nanoparticle sizes (10, 20, 30, 50 and 100 nm) were analysed as samples. A coefficient of determination greater than
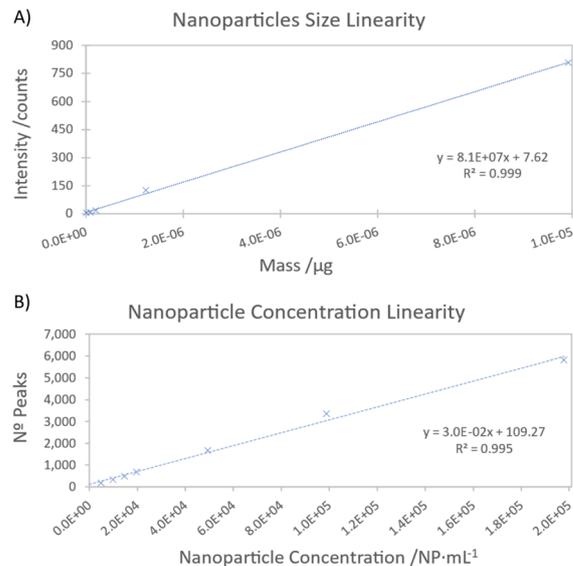

Fig. 1   Gold nanoparticle linearities. (A) Nanoparticle size; (B) nanoparticle concentration.

0.999 was obtained (Fig. 1A). To further confirm this linearity, a residual error study was conducted. Residual errors were found to be below 7% for standards between 20 and 100 nm, while the 10 nm standard exhibited a residual error of 56%. This higher error can be attributed to the proximity to the detection limit. Under these instrumental conditions, the Syngistix™ Nano Application software module provides a LOD$_{size}$ value of 13 nm by using a 3-sigma approach. This LOD$_{size}$ is
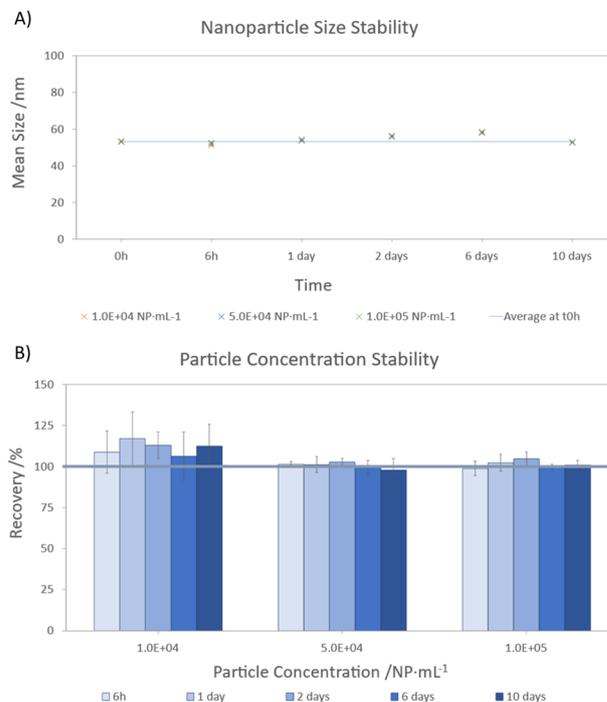
Table 1   Instrumental conditions for SP-ICP-MS analysis

Sample flow rate (mL min^{-1})	0.40 ± 0.03
Transport efficiency (%)	8.4 ± 1.0
Spray chamber	Quartz – cyclonic
Nebulizer	PFA
Cones	Pt
Plasma gas (L min^{-1})	16
Nebulizer gas (L min^{-1})	0.99
Auxiliary gas (L min^{-1})	1.2
Isotope	^{197}Au
Dwell time (µs)	50
Acquisition time (s)	60
Replicates per sample	3
Scan mode	MS/MS
Gas profile	Standard

Fig. 2   Gold nanoparticle stability in clinical diluent. (A) Nanoparticles size (mean ± s); (B) nanoparticles concentration (mean ± s).

Table 2 Blood nanoparticle characterization

| Sample ID | Nanoparticles concentration | | | Nanoparticles size | | |
	AuNP addition (NP per mL)	Nanoparticles conc. (NP per mL)	% Recovery (NP conc.)	Mean size ± 2 s (nm)	Size certified (nm)	% Error (mean size)
Blood addition 1	9890	8947	**91**	53.5 ± 0.5	49.6 ± 4.2	**7.9**
Blood addition 2	49 450	46 124	**93**	53.9 ± 0.4	49.6 ± 4.2	**8.6**
Blood addition 3	98 900	87 141	**88**	54.0 ± 0.2	49.6 ± 4.2	**8.9**

consistent with the values reported in the literature, typically ranging from 10 to 20 nm.[6,18,22,28]

In this study, we focused on AuNPs ranging from 10–100 nm, sizes commonly used in various medical applications. The ICP-MS equipment enables precise characterization of these nanoparticle sizes. This capability allows for the detection of nanoparticles, such as those preferred for cancer diagnostics due to their enhanced tumor penetration capabilities and utilization of the enhanced permeation and retention (EPR) effect.[29] Furthermore, the versatility of nanoparticle sizes enables strategic targeting in cancer therapy, where a combination of sizes can address both peripheral accumulation and deep tissue penetration within tumors. Thus, our developed method holds promise for adapting to a wider range of nanoparticle sizes, enhancing its clinical relevance.

Numerous dilutions were performed to establish the linearity range for the concentration of gold nanoparticles. A satisfactory linearity was observed within the range of 5000 to 100 000 NP per mL (Fig. 1B). The limit of detection for nanoparticle concentration was determined according to the guidelines of ISO 19590:2017, resulting in a LOD_{NP} of 147 NP per mL. This result is in agreement with the results reported by Zhang et al.,[28] who also documented an LOD_{NP} of 135 NP per mL, which indicates the consistency of the results obtained.

During the stability test, it was observed that the nanoparticle size showed consistent behaviour across all three concentration levels (Fig. 2A). However, slight variations in size were observed during storage, with deviations less than 10%. The largest difference from the initial measurement (<10%) was observed after 6 days of storage. Interestingly, despite this initial increase, the difference decreased to 1% after 10 days. This suggests that the observed variation may be due to sample introduction or insufficient stirring rather than environmental factors or interactions with the clinical diluent. For the gold nanoparticle concentration (Fig. 2B), recoveries between 95–117% were achieved. In particular, the most diluted suspensions (10^4 NP per mL) showed higher recoveries (106–117%) over time, whereas minimal differences were observed for higher AuNPs concentrations (below 5%). Despite these differences, no apparent trend of increasing or decreasing AuNPs concentration was observed over the storage period.

Therefore, these results suggest that dilution with clinical diluent and storage at 5 °C for 10 days does not adversely affect the size or concentration of these specific gold nanoparticles. Instead, the differences observed are likely to be inherent to the analytical methodology (sample preparation and instrumental technique). This highlights the feasibility of storing these nanoparticles under these conditions for subsequent analysis within this timeframe.

3.3. AuNP stability in clinical diluent

Three stability tests were performed at different concentrations (10^4, 5×10^4 and 10^5 NP per mL) to investigate the behaviour of AuNPs when exposed to the clinical diluent. Freshly prepared samples (t_{0h}) and samples stored for 6 hours (t_{6h}), 1 (t_{1d}), 2 (t_{2d}), 6 (t_{6d}) and 10 days (t_{10d}) were analysed. The results for AuNP size and concentration are shown in Fig. 2. These results were compared with those obtained at t_{0h} to assess the variations in the nanoparticle size and concentration over the specified period.

3.4. Method suitability for AuNP characterization in blood and urine

The suitability of the developed methodology for gold nanoparticles characterization in blood and urine using SP-ICP-MS was evaluated. As described in Section 2.3, gold nanoparticle standards (50 nm) were added to blood and urine at three different concentrations as a model analyte.

Sizes between 53.5 and 54.0 nm were obtained when characterizing the size of gold nanoparticles in the blood (Table 2). Compared to the certified values (49.6 ± 4.2 nm), a maximum

Table 3 Urine nanoparticle characterization

| Sample ID | Nanoparticles concentration | | | Nanoparticles size | | |
	AuNP addition (NP per mL)	Nanoparticles conc. (NP per mL)	% Recovery (NP conc.)	Mean size ± 2 s (nm)	Size certified (nm)	% Error (mean size)
Urine addition 1	9890	9441	**96**	49.2 ± 0.3	49.6 ± 4.2	**−0.7**
Urine addition 2	49 450	50 411	**102**	49.6 ± 0.2	49.6 ± 4.2	**0.1**
Urine addition 3	98 900	101 359	**103**	50.0 ± 0.3	49.6 ± 4.2	**0.9**

This journal is © The Royal Society of Chemistry 2024

J. Anal. At. Spectrom., 2024, **39**, 2508–2513 | **2511**

difference of 8.9% was observed. A t-student test was performed, and no significant difference was observed ($p > 0.05$). However, a slight increase in the signal of the gold nanoparticles in blood cannot be ruled out, which may lead to a bias towards larger sizes. Despite a lower concentration of gold nanoparticles detected in blood compared to the added concentration, recoveries between 88–93% were achieved (t-student test: $p > 0.05$ for all cases), indicating a uniform recovery efficiency independent of the nanoparticle concentration.

Similarly, the same procedure was followed to assess the suitability of the method for gold nanoparticle characterization in urine (Table 3). In this case, the nanoparticle size values ranged from 49.2 to 50.0 nm, practically matching the certified values (49.6 ± 4.2 nm). Good recoveries were obtained for the gold nanoparticle concentration (between 90 and 95%), suggesting no significant matrix effects (t-student test: $p > 0.05$ in all cases). To summarize, the results demonstrate the reliability and consistency of the characterization methodology used in this study, highlighting its suitability for characterizing gold nanoparticles in both blood and urine matrices.

4. Conclusions

This study evaluated the suitability of the clinical diluent for the characterization of gold nanoparticles in blood and urine using SP-ICP-MS. Several analytical parameters were investigated, including linearity, where coefficients of determination higher than 0.995 were obtained for both the dissolved gold and nanoparticles (size and concentration). In addition, detection limits were determined, resulting in values of 0.012 μg L^{-1} for dissolved gold, 13 nm for the nanoparticle size and 147 NP per mL for nanoparticle concentration.

An assessment of whether the clinical diluent could affect the gold nanoparticles was also made. It was observed that after 10 days of storage at 5 °C, both AuNP size and concentration were unaffected, with differences of less than 10% and recoveries between 95–117%.

The behaviour of gold nanoparticles was also investigated when spiked into blood and urine and characterized by direct dilution with clinical diluent. Notably, differences of less than 9% were observed for nanoparticle size with respect to the certified value, along with recoveries of 88–103% for total nanoparticle concentration in both matrices.

Based on these results, it can be concluded that clinical diluent is a suitable solution for characterizing gold nanoparticles in blood and urine under these conditions. This underlines the usefulness of clinical diluent as a matrix diluent for analysing nanoparticles in biological samples.

List of abbreviations

AF4-ICP-MS	Asymmetric Flow Field-Flow Fractionation coupled to Induction Coupled Plasma-Mass Spectrometry
AuNPs	Gold nanoparticles
DLS	Dynamic Light Scattering
EDTA	Ethylenediaminetetraacetic acid
ICP-MS	Inductively Coupled Plasma – Mass Spectrometry
LOD$_{NP}$	Detection limit for nanoparticle concentration
LOD$_{size}$	Detection limit for nanoparticle size
NPs	Nanoparticles
NTA	Nanoparticle Tracking Analysis
SEM	Scanning Electron Microscopy
SP-ICP-MS	Single Particle-Inductively Coupled Plasma-Mass Spectrometry
TEM	Transmission Electron Microscopy

Data availability

Data are available at https://dataverse.csuc.cat/dataverse/URL.

Author contributions

Meritxell Cabré: investigation, methodology, validation, writing-original draft and writing–review and editing. Gabriel Fernández: investigation, methodology, validation, writing-original draft. Esther González: resources, visualization, and writing – review and editing. Jordi Abellà: conceptualization, funding acquisition, project administration, supervision, visualization, and writing – review and editing. Ariadna Verdaguer: conceptualization, funding acquisition, methodology, project administration, resources, supervision, visualization, and writing – review and editing.

Conflicts of interest

The authors declare that they have no known competing financial interests or personal relationships that could have appeared to influence the work reported in this paper.

Acknowledgements

References

1 L. Leon, E. J. Chung and C. Rinaldi, in *Nanoparticles for Biomedical Applications: Fundamental Concepts, Biological Interactions and Clinical Applications*, Elsevier Inc., 2020, pp. 1–4.

2 C. Enrico, in *Design of Nanostructures for Theranostics Applications*, William Andrew Publishing, 2018, pp. 41–68.

3 X. Y. Wong, A. Sena-Torralba, R. Álvarez-Diduk, K. Muthoosamy and A. Merkoçi, *ACS Nano*, 2020, **14**, 2585–2627.

4 M. Nikzamir, A. Akbarzadeh and Y. Panahi, *J. Drug Delivery Sci. Technol.*, 2023, **61**, 102316.

5 N. Sarfraz and I. Khan, *Chem.–Asian J.*, 2021, **16**, 720–742.

2512 | *J. Anal. At. Spectrom.*, 2024, **39**, 2508–2513

This journal is © The Royal Society of Chemistry 2024

6 S. Fernandez Trujillo, M. Jimenez Moreno, A. Ríos and R. D. C. Rodríguez Martín-Doimeadios, *J. Anal. At. Spectrom.*, 2021, **36**, 528–534.

7 S. J. Soenen, W. J. Parak, J. Rejman and B. Manshian, *Chem. Rev.*, 2015, **115**, 2109–2135.

8 C. Soica, I. Pinzaru, C. Trandafirescu, F. Andrica, C. Danciu, M. Mioc, D. Coricovac, C. Sitaru and C. Dehelean, in *Design of Nanostructures for Theranostics Applications*, Elsevier, 2018, pp. 161–242.

9 M. G. Soliman, P. del Pino, W. J. Parak and B. Pelaz, in *Reference Module in Chemistry, Molecular Sciences and Chemical Engineering*, Elsevier, 2017.

10 O. A. Sadik, N. Du, V. Kariuki, V. Okello and V. Bushlyar, in *ACS Sustainable Chemistry and Engineering*, American Chemical Society, 2014, vol. 2, pp. 1707–1716.

11 F. Barbero, C. Mayall, D. Drobne, J. Saiz-Poseu, N. G. Bastús and V. Puntes, *Sci. Total Environ.*, 2021, **768**, 144792.

12 M. Logozzi, D. Mizzoni, B. Bocca, R. Di Raimo, F. Petrucci, S. Caimi, A. Alimonti, M. Falchi, F. Cappello, C. Campanella, C. C. Bavisotto, S. David, F. Bucchieri, D. F. Angelini, L. Battistini and S. Fais, *Eur. J. Pharm. Biopharm.*, 2019, **137**, 23–36.

13 R. S. Amais, G. L. Donati and M. A. Zezzi Arruda, *Trends Anal. Chem.*, 2020, **133**, 116094.

14 R. M. Galazzi, K. Chacón-Madrid, D. C. Freitas, L. F. da Costa and M. A. Z. Arruda, *Rapid Commun. Mass Spectrom.*, 2020, **34**, 1–14.

15 W. Liu, H. Shi, K. Liu, X. Liu, E. Sahle-Demessie and C. Stephan, *J. Agric. Food Chem.*, 2021, **69**, 1115–1122.

16 C. Degueldre and P. Y. Favarger, in *Colloids and Surfaces A: Physicochemical and Engineering Aspects*, Elsevier, 2003, vol. 217, pp. 137–142.

17 O. V. Kuznetsova, G. M. D. M. Rubio, B. K. Keppler, J. M. Chin, M. R. Reithofer and A. R. Timerbaev, *Anal. Biochem.*, 2020, **611**, 114003.

18 J. Liu, K. E. Murphy, R. I. Maccuspie and M. R. Winchester, *Anal. Chem.*, 2014, **86**, 3405–3414.

19 H. E. Pace, N. J. Rogers, C. Jarolimek, V. A. Coleman, C. P. Higgins and J. F. Ranville, *Anal. Chem.*, 2011, **83**, 9361–9369.

20 C. Degueldre, P. Y. Favarger and S. Wold, *Anal. Chim. Acta*, 2006, **555**, 263–268.

21 J. Campbell, S. Burkitt, N. Dong and C. Zavaleta, in *Nanoparticles for Biomedical Applications: Fundamental Concepts, Biological Interactions and Clinical Applications*, Elsevier Inc., 2020, pp. 129–144.

22 F. Laborda, E. Bolea and J. Jiménez-Lamana, *Anal. Chem.*, 2013, **86**, 2270–2278.

23 H. Goenaga-Infante and D. Bartczak, in *Characterization of Nanoparticles: Measurement Processes for Nanoparticles*, Elsevier, 2019, pp. 65–77.

24 E. Bolea-Fernandez, D. Leite, A. Rua-Ibarz, T. Liu, G. Woods, M. Aramendia, M. Resano and F. Vanhaecke, *Anal. Chim. Acta*, 2019, **1077**, 95–106.

25 Y. Lu, M. Kippler, F. Harari, M. Grandér, B. Palm, H. Nordqvist and M. Vahter, *Clin. Biochem.*, 2015, **48**, 140–147.

26 F. Laborda, A. C. Gimenez-Ingalaturre, E. Bolea and J. R. Castillo, *Spectrochim. Acta, Part B*, 2020, **169**, 105883.

27 F. Laborda, J. Jiménez-Lamana, E. Bolea and J. R. Castillo, *J. Anal. At. Spectrom.*, 2013, **28**, 1220–1232.

28 X. He, H. Zhang, H. Shi, W. Liu and E. Sahle-Demessie, *J. Am. Soc. Mass Spectrom.*, 2020, **31**, 2180–2190.

29 E. Casals, G. Casals, V. Puntes and J. M. Rosenholm, in *Theranostic Bionanomaterials*, Elsevier, 2019, pp. 3–26.

This journal is © The Royal Society of Chemistry 2024

J. Anal. At. Spectrom., 2024, **39**, 2508–2513 | **2513**